In Vivo Static and Dynamic Lengthening Measurements of the Posterior Cruciate Ligament at High Knee Flexion Angles

Caecilia Charbonnier[1-2], PhD, Victoria B. Duthon[3], MD, Sylvain Chagué[1], MS, Frank C. Kolo[4], MD, Jacques Ménétrey[3], MD

Medical Research Department, Artanim Foundation, Geneva, Switzerland[1]

Faculty of Medicine, University of Geneva, Geneva, Switzerland[2]

Centre de médecine du sport et de l'exercice, Hirslanden Clinique La Colline, Geneva, Switzerland[3]

Rive Droite Radiology Center, Geneva, Switzerland[4]

Conflict of Interest: The authors declare that they have no conflict of interest.

Corresponding author:

Caecilia Charbonnier, PhD, PD
Artanim Foundation
40, chemin du Grand-Puits – 1217 Meyrin, Switzerland
Telephone number: +41 22 980 91 92
E-mail address: caecilia.charbonnier@artanim.ch

Abstract

Purpose: Rehabilitation is an important aspect of both nonoperative and operative treatment of knee ligaments tear. Posterior cruciate ligament (PCL) non-operative treatment consists of a step-by-step rehabilitation protocol and is well described. It goes from rest (phase I) to strengthening exercises (phase IV). More specific and high intensity exercises such as cutting, sidestepping or jumps are however not described in detail, as no in vivo data exist to tell how these exercises constrain the ligaments and if they have the same effect on all of them, in particular regarding lengthening. The goal of this study was to measure the ligament lengthening in static knee flexion based on 3D reconstructions from Magnetic Resonance Imaging (MRI), and from motion capture and ligament simulation during dynamic exercises.

Methods: The knee of nine volunteers was first imaged in a close-bore MRI scanner at various static knee flexion angles (up to 110°) and the corresponding lengthening of the PCL and the other major knee ligaments was measured. Then, the volunteers underwent motion capture of the knee where dynamic exercises (sitting, jumping, sidestepping, etc.) were recorded. For each exercise, knee ligaments elongation was simulated and evaluated.

Results: According to the MRI scans, maximal lengthening occurred at 110° of flexion in the anterior cruciate ligament (ACL) and 90° of flexion in the PCL. Daily living movements such as sitting were predicted to elongate the cruciate ligaments, whereas they shortened the collateral ligaments. More active movements such as jumping put the most constrain to cruciate ligaments.

Conclusion: This study provides interesting insights for a tailored post-operative regimen. In particular, knowing the knee ligaments lengthening during dynamic exercises can help better define the last stages of the rehabilitation protocol, and hence provide a safe return to play.

Keywords: Posterior cruciate ligament; Knee ligaments lengthening; High knee flexion; MRI; Motion capture; Kinematics; Simulation.

Word count: 3541

Introduction

Rehabilitation is an important aspect of both nonoperative and operative treatment of knee ligaments tear. Knee ligaments reconstruction is successful if a specific rehabilitation program is conducted after the surgery. The goal of this program is to recover knee range of motion (ROM) and function, without constraining too much the graft or the torn ligament in order to let it heal and to prevent graft loosening. Thus, knowing the biomechanical behavior of the ligaments and their lengthening are mandatory, not only during basic ROM but also during specific rehabilitation exercises, such as jumps or squats. Knee ligaments properties and behavior have been largely studied in labs on cadaveric knees. The posterior cruciate ligament (PCL) is the primary restraint to posterior tibial translation and consists of two components, the anterolateral and posteromedial bundles which demonstrate different strains at different degrees of knee flexion [3, 5]. Cadaveric studies have also analyzed the tensile strength, chondral deformation forces, and primary and secondary restraining functions of the PCL [5].

All rehabilitation protocols are based on these laboratory data, by extrapolating the results. But do live exercises constrain the ligaments exactly the same way as in the experiments? Komatsu et al. [18] showed that the PCL played an important role for the maintenance of the joint gap during flexion in Magnetic Resonance Imaging (MRI) from extension to deep flexion. Goyal et al. [14] used Dynamic Stereo X-Ray (DSX) and showed that patients with isolated PCL injuries experienced significant knee instability during running and stair ascent that could not be identified by standard non-weight bearing static laxity measurements. The findings that different activities create different degrees of instability may have important implications for rehabilitation and activity limitations for PCL-deficient individuals [14].

PCL non-operative treatment consists of a step-by-step rehabilitation protocol and is well described. It goes from rest (phase I) to strengthening exercises [1, 16, 19, 23] (phase IV). More specific and high intensity exercises such as cutting, sidestepping or jumps are not described in detail in such rehabilitation protocols, as no in vivo data exist to tell how these exercises constrain these ligaments and if they have the same effect on all of them, in particular regarding lengthening. Studying the dynamic behavior of the knee ligaments during daily living and high intensity exercises could hence improve the rehabilitation protocols.

From a static point of view, MRI is ideal for studying the knee ligaments, because this modality offers a good visibility of these tissues. However, only few studies [28, 29, 35] have succeeded in imaging the knee in up to 90° flexion in close-bore MRI scanners, due to the limited space to position the patient. Open-bore MRI scanners allow knees to be imaged at higher ROMs [10, 17, 18, 22] but generally with lower signal-to-noise ratio, resulting in decreased image quality. Nevertheless, studying knee ligaments deformation based on MRI remains difficult due to the complex technical protocol. Therefore, data about mechanical and morphological changes in knee ligament measured in vivo is still sparse.

3D simulation techniques, combining both anatomical and kinematical models of the patient, can be good solutions to obtain a more comprehensive understanding of the knee joint biomechanics. However, simulating ligament deformation during motion and thus measuring elongation in vivo are challenging. Current physically-based methods (e.g., finite element models, musculoskeletal models) are difficult to set up or are limited to simple knee motion simulation where loads can be estimated [2, 15, 25, 30, 33]. In this study, we hence propose the use of a simplified technique [7] based on a patient-specific bone-ligament representation which allows stable and real-time simulation of the knee ligaments during complex motion, such as strengthening exercises.

The aim of this study was twofold. First, to image in a close-bore MRI scanner the PCL and the other major knee ligaments to measure their corresponding lengthening at various static knee flexion angles up to 110°. Our hypothesis was that the PCL has a curved shape in extension and straighten in flexion. The second objective was to simulate and evaluate knee ligaments elongation during dynamic exercises (e.g., sitting, jumping, sidestepping) recorded by motion capture, in order to fine tune the rehabilitation program and to grade these dynamic movements in terms of ligament solicitation. We expected similar lengthening patterns compared to the static MRI study but of increased magnitude due to the velocity of the movements.

Methods

Subjects

The measurements were made on the right knee of nine healthy young active participants (five females, four males). The mean age, weight and height were 27.2 years, 63.2 kg and 167.4 cm, respectively. Because of the MRI technical protocol, a height criterion was used. The subjects higher than 180 cm were excluded. Other exclusion criteria were reported previous knee injuries, knee surgery or contraindications for MRI. Institutional ethical approval (CCER n°15-043) was obtained prior to data collection. All procedures performed in the study were in accordance with the ethical standards of the institutional and/or national research committee and with the 1964 Helsinki declaration and its later amendments or comparable ethical standards. Informed consent was obtained from all participants included in the study.

MRI acquisition and morphological evaluation

All volunteers were MRI scanned with a 1.5 T Optima MR450w GEM system (General Electric Healthcare, Milwaukee, WI, USA). A flexible surface coil was used and images were acquired at several unloaded knee flexions: 0°, 45°, 90° and 110°. At neutral knee flexion (0°), the subjects were placed in supine position. One 3D intermediate weighted fast spin echo without fat saturation (Cube®) sequence (section thickness 0.8 mm; no gaps; TR/TE ms 1500/27.9) centered on the knee and three 3D fast gradient echo (Lava®) sequences (section thickness 3 mm; no gaps; TR/TE ms 4.2/2.0) were achieved covering a region of interest from the pelvis to the ankle. For the other flexion angles, the subjects were lying on the right side to ensure sufficient room to center the knee joint in the magnetic bore (Figure 1). A hand-held goniometer was used to position the subject's lower limb at the desired knee flexion. For each position, one 3D intermediate weighted fast spin echo without fat saturation (Cube®) sequence was acquired.

Figure 1. Subject lying on the right side with the knee flexed at 90° for MRI scan.

A musculoskeletal radiologist (FCK) with 13 years of experience assessed all MR images in each degree of flexion. For each volunteer, signal, orientation and morphology of each ligamentous and tendinous structure was assessed. The shape and direction of the PCL was also especially evaluated and abnormal signal and morphology of the ligament was reported. Bony morphology and associated lesion of articular structures as cartilage and menisci were also documented.

3D reconstruction and ligaments measurements at MRI

Bone geometry was obtained from 3D reconstruction based on the 3D images in neutral knee flexion. The MRI volumes were registered and manually segmented using Mimics software (Materialize NV, Leuven, Belgium). For each volunteer, subject-specific 3D models of the femur, tibia, fibula and patella were thus obtained. For reference, the 3D bone models were also registered to each MRI pose. The knee ligaments (PCL, anterior cruciate ligament (ACL), medial collateral ligament (MCL) and lateral collateral ligament (LCL)) were reconstructed for each flexion angle based on the high-resolution 3D Cube® images and modelled as 3D splines centered on the ligament's medial axis (Figure 2). Since anatomically and biomechanically differences between the PCL fiber bundles have been reported [3, 19], both the anterolateral (PCL_AL) and posteromedial (PCL_PM) fiber bundles were reconstructed. However, we did not reconstruct the two fiber bundles of the ACL (anteromedial and posterolateral), because this ligament was well studied in previous researches [15, 30] and was not the main focus of our study.

The 3D splines were used to measure the ligament length at the different knee flexion angles (0°, 45°, 90°, 110°). For clarity, the obtained measures were also expressed as a percentage of elongation or shortening (ratio of current length in millimeter with respect to the base length in neutral flexion, expressed in %).

Motion recording and kinematic modeling

Following MRI scan, the volunteers participated to a motion capture session. They were equipped with a dedicated knee markers protocol [6] (see Figure 3), including twelve spherical retroreflective markers (Ø 14 mm) placed directly onto the skin using double sided adhesive tape. The femur marker set included three markers placed on anatomical landmarks (greater trochanter, lateral and medial femoral epicondyles) and four markers distributed on the lateral and frontal parts of the thigh. For the tibia/fibula, three markers were placed on anatomical landmarks (tibial tuberosity, medial and lateral malleoli), one on the lateral part and one on the medial part of the shank. Additional markers were distributed over the body (trunk, upper limbs, contralateral leg and feet) to provide a global visualization of the motion.

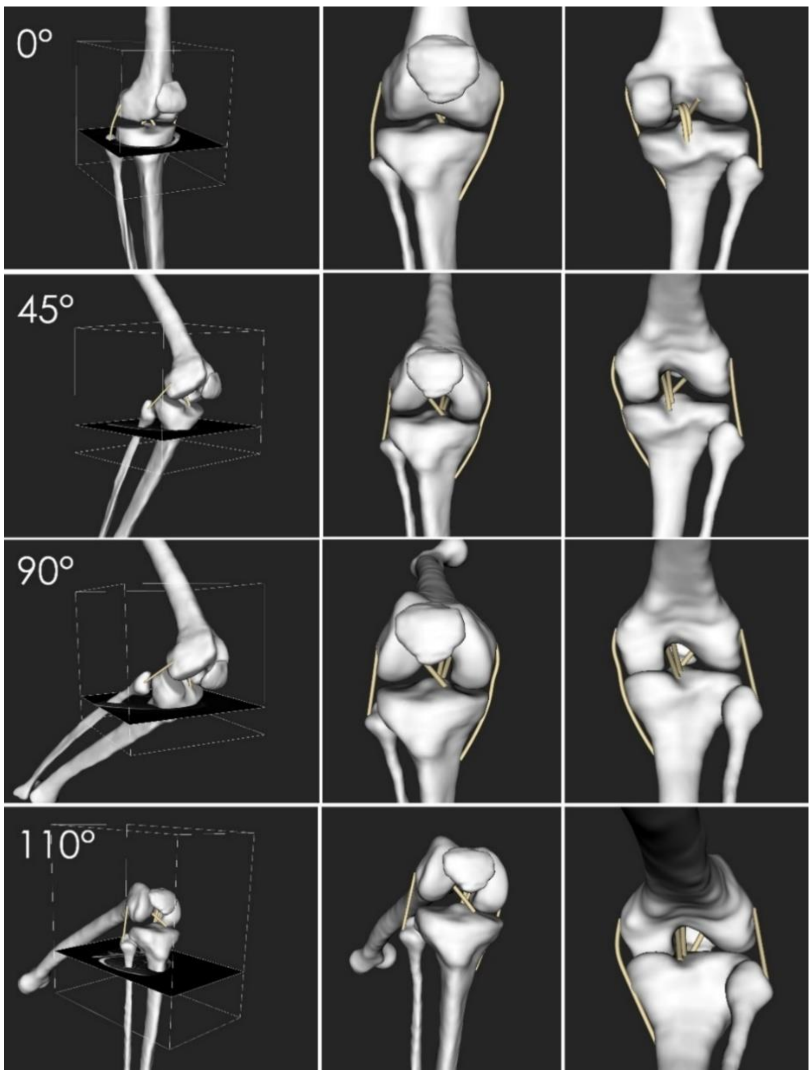

Figure 2. 3D bone models reconstructed in neutral knee flexion and registered to each MRI pose with the reconstructed ligaments as 3D splines (left, knee poses with the high-resolution 3D Cube® images; middle, anterior view; right, posterior view).

After appropriate warm-up, the volunteers were asked to perform three trials of the following dynamic activities: 1) sitting on a low seat, 2) cutting motion, 3) drop jump from a 45 cm height stool followed by a kangaroo jump, and 4) sidestepping from one direction to the other with the knees flexed at a minimum of 50°-60° during approximatively 30 seconds. These activities were chosen, because they all required important knee flexion and mostly at a high velocity, and because they are part of the last steps of any rehabilitation program after ligament reconstruction. Motion was recorded using a Vicon MXT40S motion capture system (Vicon, Oxford Metrics, Oxford, UK) consisting of twenty-four cameras sampling at 120Hz. The same investigator (CC) attached all markers and performed all measurements.

Knee kinematics were computed from the markers trajectories based on the definitions suggested by the International Society of Biomechanics [34] and using a validated biomechanical model [6] which accounted for skin motion artifacts (accuracy: translational error <3 mm, rotational error <6°). The model was based on multi-body optimization (MBO) [8, 9, 13, 20, 26, 27] with a personalized parallel mechanism (i.e., four ligaments constraints with prescribed ligament length variations and two surface-on-plane contacts defined on the subject-specific knee models). The main advantage of such parallel mechanism is its ability to realistically model the complex physiological kinematic behavior of the knee that comes into play at high ROM (i.e., knee rollback) [6, 11, 20]. More details about the model and its validation can be found in Charbonnier et al. [6]. As a result, the subject's knee 3D models could be visualized at each point of the movement (Figure 3).

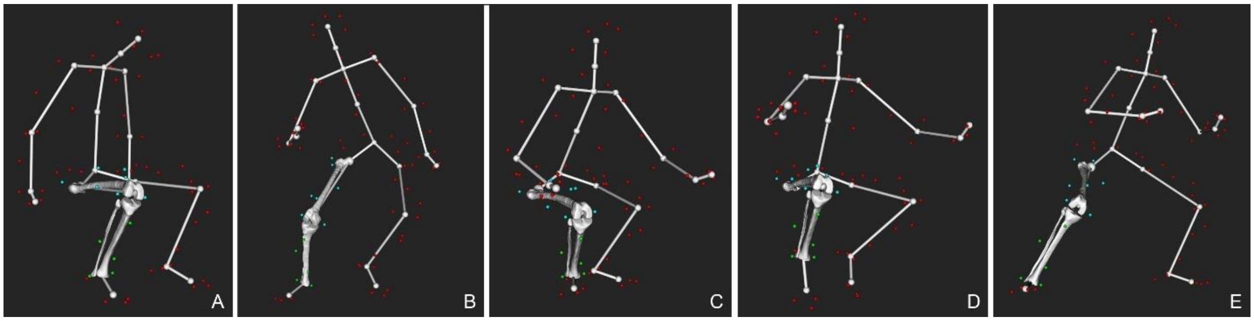

Figure 3. Examples of computed postures showing the markers set-up (small colored spheres) and a virtual skeleton used to better visualize and analyze the motion as a whole: A) sitting on a low seat (maximal knee flexion), B) cutting motion (maximal knee flexion while changing of direction), C) drop jump (maximal knee flexion during reception), D) kangaroo jump (maximal knee flexion while jumping), and E) sidestepping.

Ligaments simulation and evaluation of elongation during motion

Once knee kinematics were computed, ligaments were subsequently simulated using a position-based dynamics approach [7, 21]. This simulation technique was developed and described in a previous study assessing rotator cuff elongation during shoulder strengthening exercises obtained from motion capture data [7]. In summary, the 3D splines are first discretized into a set of connected particles. Then, position-based dynamics directly derive position updates from the particle positions itself using a straight-forward distance constraint which attempts to keep the distance between two particles equal to a specified rest-length. This simple formulation allows for real-time evaluation of the simulation, while remaining inherently stable. To prevent interpenetration between the 3D bone models and the splines, continuous collision detection is used [24] in combination with an AABB tree [4] to speed up the computation in an efficient way.

To validate the simulation technique in the present ligament context, the ligaments lengths computed by the simulation were compared with those measured on the MRI at the different knee flexion angles (45°, 90° and 110°). This was achieved by using the position and orientation of the 3D bone models registered to each MRI pose as input in the simulation [7] and the 3D splines of the ligaments reconstructed for each MRI pose as reference lengths (see Figure 2).

The proposed simulation technique was then used to compute ligaments lengths during the dynamic exercises recorded by motion capture. For the sidesteps, the measures were taken during the entire ROM and averaged. For the other movements, the measures were taken at critical positions (see Figure 3): for sitting at maximal knee flexion, for cutting at maximal knee flexion while changing of direction, for the drop jump at maximal knee flexion during reception, and for the kangaroo jump at maximal knee flexion while jumping. The measures were expressed as a percentage of elongation (or shortening) with respect to the ligament length at neutral flexion. Moreover, a color scale was used to visualize the length variations of the 3D splines, with warm colors denoting elongation and cool colors indicating shortening (Figure 4).

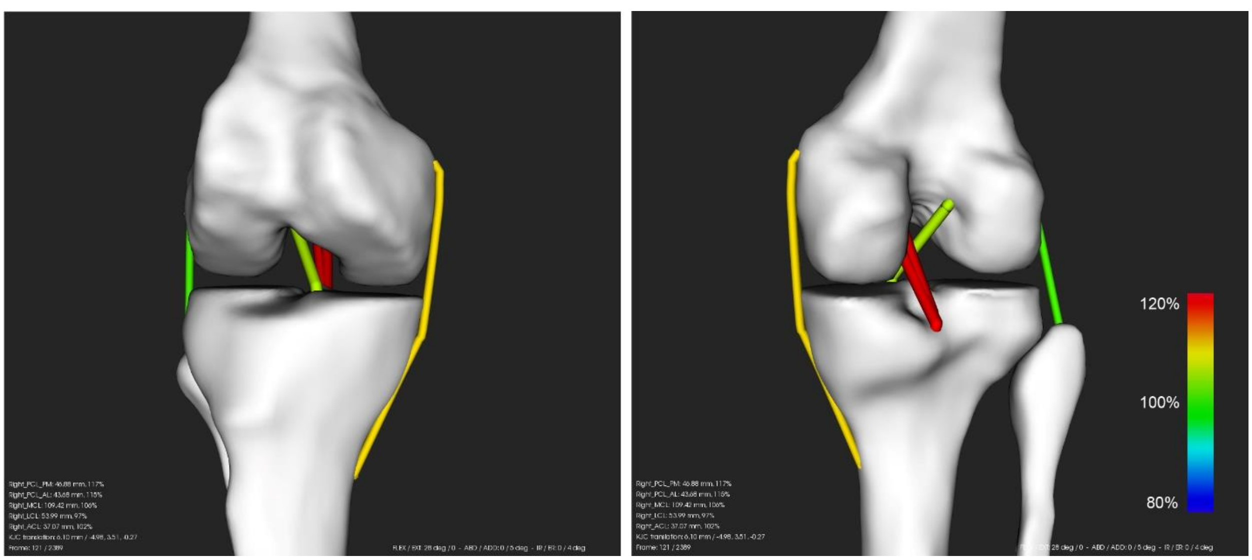

Figure 4. Ligaments simulation (front and back views). The colors represent the length variations with respect to the neutral knee pose: warm colors mean that the ligament is elongated, whereas cool colors mean that the ligament is shortened during motion.

Statistical analysis

Descriptive statistics are presented as mean and standard deviations (SD). For each subject, we calculated based on the 3D reconstructions from MRI the ligaments length variation at the different knee flexion angles. For each dynamic activity and for each trial, we calculated at critical positions the length variation for each ligament. For the validation of the ligament simulation technique, we calculated the errors between the ligaments lengths computed by the simulation with those measured on the MRI at the different knee flexion angles.

Results

Morphological findings

Among all the volunteers, evaluation of the MR images revealed two of them showing superficial fraying of the patellar cartilage. No other lesions were found. Based on the 3D Cube® images, the analysis of the posterior cruciate ligament did not show any pathology. The PCL was smooth and continuous with homogenous hypo-intensity on all sequences acquired. No thickening was noted on the images acquired at neutral knee flexion. Images acquired with the most important degrees of flexion showed a thinner and elongated PCL but no abnormal signal was noted.

Ligaments lengths at MRI

As shown in Figure 5, ACL shortened from 0° until 45° of knee flexion (mean ± SD: 96% ± 5%) and then slightly lengthened with increasing flexion (mean ± SD: 100% ± 5% at 90°, 106% ± 7% at 110°). PCL presented a curved shape below 45° of knee flexion, lengthened maximally around 90° and then shortened until 110°. PCL_PM length was in average longer than PCL_AL: respectively, 105% ± 6% and 105% ± 5% at 45°, 109% ± 5% and 108% ± 6% at 90°, and 108% ± 6% and 106% ± 7% at 110°. Concerning MCL and LCL, they constantly shortened from 0° until 110° of knee flexion. Table 1 summarizes the ligaments lengths and their variation measured based on 3D reconstructions from MRI.

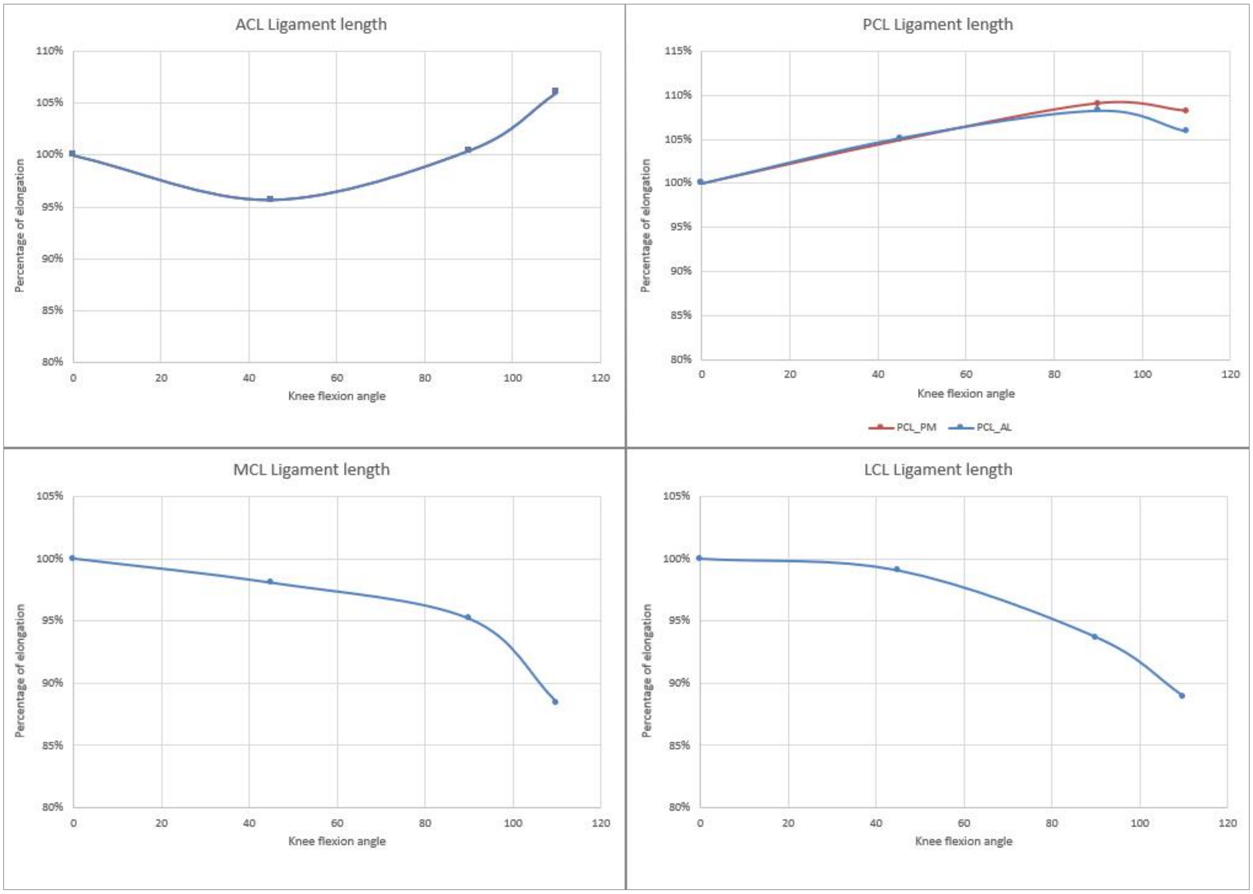

Figure 5. Average percentage of elongation of the knee ligaments in function of the knee flexion angles (n = 9).

Ligaments lengths during dynamic activities

Ligament lengths computed by the simulation showed good agreement with respect to MRI measurements in the different knee flexion angles (Table 2) but were always slightly overestimated. The simulated MCL and LCL presented small length errors (mean ratio: 1% and 4%, respectively), while the ACL, PCL_PM and PCL_AL lengths were slightly more overestimated by the simulation (mean ratio: 7%, 7% and 6%, respectively).

Ligament length variations were estimated to vary from 88% to 123% in average during the various dynamic exercises (Table 3). The ACL and PCL elongated in all activities (range: 108-115% for ACL, 111-117% for PCL_PM and 114-123% for PCL_AL) with maximal elongations during movements requiring more knee flexion (sitting in a low seat, drop jump and kangaroo jump). The anterolateral fiber bundle of the PCL always lengthened more than the posteromedial fiber bundle. MCL and LCL showed less pronounced patterns of length variations (range: 88-102% and 93-100%, respectively) but globally increased shortening with movements requiring more knee flexion.

Discussion

This study measured the ligament lengthening in static knee flexion based on 3D reconstructions from MRI, and from motion capture and ligament simulation during dynamic exercises.

The results of this study revealed that the cruciate ligaments were not isometric structures. According to the MRI scans, ACL shortened from 0° until 45° of knee flexion and then slightly lengthened with increasing flexion. Maximal lengthening occurred at 110° of flexion in the ACL. PCL presented a curved shape below 45° of knee flexion, lengthened maximally around 90° and then shortened until 110°. Simulation and evaluation of knee ligament elongation correlated reliably with MRI measurements. Dynamically, the AL fiber bundle compared to the PM fiber bundle of PCL showed the greatest lengthening variations according to the movements performed. PCL and ACL were maximally elongated during kangaroo jumps. MCL was maximally elongated during sidestepping, and LCL was maximally elongated during cutting movements.

The outcomes also provided interesting insights to better define the post-operative rehabilitation protocols. Daily living movements as sitting were predicted to elongate the cruciate ligaments, whereas they shortened the collateral ligaments. Cutting movements elongated ACL and PCL much more than MCL and LCL. Drop jump and kangaroo jump put the most constrain to cruciate ligaments and this was maximal during kangaroo jump. Sidestepping elongated the ACL, PCL and MCL, but not the LCL. Based on these findings, ACL and PCL reconstruction should be initially rehabilitate in the first degrees of flexion, whereas MCL and LCL patients can be moved to cutting activities sooner without harm. Jumps, especially drop and kangaroo jump, should not be performed before the ending rehabilitation phase. Sidestepping is part of the return to sport testing battery and the high constrain measured during this maneuver should caution its use too early into the post-operative period. Even sitting in a deep armchair after a PCL reconstruction should not be recommended before the proper healing and incorporation of the graft (probably 6 months).

Compared to the literature, our results are in agreement with previous in vivo works. Utturkar et al. [32] measured ACL elongation using MRI and biplanar fluoroscopy during static knee positions, and showed a decreased of the ACL length from full extension to 30° of flexion as observed in the present study. They however did not image the knee at higher flexion angles. King et al. [17] measured PCL lengthening during flexion using an open-bore MRI scanner. The PCL appeared curved when the knee was in unloaded relaxed extension and appeared straight at 40° of flexion. The study also depicted similar lengthening patterns of the anterior surface of the PCL between extension and 120° of flexion. Regarding dynamic activities, Englander et al. [12] and Taylor et al. [31] measured ACL elongation during single-legged jump and jump landing, respectively, using a combination of MRI, biplanar fluoroscopy and motion capture. In both cases, the jumps under evaluation did not exceed 20-45° of knee flexion. The authors concluded that the length of the ACL during these activities decreased with increasing flexion angle, which corresponds to our MRI observations at low flexion angles. We did not find any study measuring knee ligaments elongation during dynamic activities at high knee flexion angles like the ones investigated in our study.

Although the simulation technique presented in this paper is a simplified non-physical approach, it is based on a patient-specific bone-ligament representation enabling a stable and real-time simulation of the knee ligaments during complex motion, thus allowing gathering valuable clinical data. In particular, this study offers novel insights into the analysis of mechanical and morphological changes in knee ligaments measured in vivo at different knee flexion angles and both statically and dynamically.

There were several limitations that warrant discussion. First, the accuracy of the kinematics computation from motion capture data could be criticized. Indeed, the model based on MBO did not account for muscle dynamics and its validation was obtained against MRI during static and non-weight-bearing knee poses. Tibio-femoral orientation and translation errors were reported to be respectively within 6° and 3 mm for each anatomical plane [6], which is acceptable for clinical use in the study of knee physiology and pathology, but one should acknowledge that the accuracy of this model may vary when considering dynamic activities. Second, our proposed techniques are non-physical and irrespective of many loads, as no physical model allowing simulation of knee ligament elongation in such complex motions exists. Moreover, the validation of the ligament simulation was based on static MRI knee poses, which does not represent dynamic activities. It is also important to note that we would have been unable to evaluate the PCL below 45° of knee flexion, as at these degrees this ligament presents a curved shape – a behavior we cannot simulate due to the nature of the simulation technique that tries to find the shortest path between the two attachment points. Nevertheless, this study was interested in measuring ligament lengthening at higher knee flexion degrees. Third and last, the static ligament length measurements were based on 3D splines, a simplified 3D reconstruction. Reconstructing the entire surfacic mesh would provide more accurate measurements but would also require accurate ligament segmentation on medical images, which remains a complicated task.

Future work should consider the evaluation of additional healthy subjects, as well as post-operative patients, as findings may be different in knees with pathology. Further strengthening exercises should also be investigated to propose comprehensive recommendations for the design of knee strength training protocols.

Conclusion

The experimental and simulation results of this study are in agreement with previous biomechanical and imaging studies and provide interesting insights for a tailored post-operative regimen. Statically, ACL and PCL were maximally lengthened at 110° and 90° of knee flexion, respectively. Dynamically, cruciate ligaments were estimated to elongate during daily living movements such as sitting, whereas collateral ligaments shortened. More active movements such as jumping put the most constrain to cruciate ligaments. Knowing the knee ligaments lengthening during dynamic exercises can help better define the last stages of the rehabilitation protocol, and hence provide a safe return to play.

Research involving humans: Institutional ethical approval (CCER n°15-043) was obtained prior to data collection. All procedures performed in the study were in accordance with the ethical standards of the institutional and/or national research committee and with the 1964 Helsinki declaration and its later amendments or comparable ethical standards. Informed consent was obtained from the individual participant included in the study.

References

1. Agolley D, Gabr A, Benjamin-Laing H, Haddad F (2017) Successful return to sports in athletes following non-operative management of acute isolated posterior cruciate ligament injuries: medium-term follow-up. Bone Joint J 99-B(6):774–778

2. Ali A, Harris M, Shalhoub S, Maletsky L, Rullkoetter P, Shelburne K (2016) Combined measurement and modeling of specimen-specific knee mechanics for healthy and ACL-deficient conditions. J Biomech 24(57):117–124

3. Amis A, Bull A, Gupte C, Hijazi I, Race A, Robinson J (2003) Biomechanics of the PCL and related structures: posterolateral, posteromedial and meniscofemoral ligaments. Knee Surg Sport Traumatol Arthrosc 11(5):271–281

4. van den Bergen G (1997) Efficient collision detection of complex deformable models using AABB trees. J Graphics Tools 2(4):1–14

5. Chandrasekaran S, Ma D, Scarvell J, Woods K, Smith P (2012) A review of the anatomical, biomechanical and kinematic findings of posterior cruciate ligament injury with respect to non-operative management. Knee 19(6):738–745

6. Charbonnier C, Chagué S, Kolo F, Duthon V, Menetrey J (2017) Multi-body Optimization with Subject-Specific Knee Models: Performance at High Knee Flexion Angles. Comput Meth Biomech Biomed Eng 20(14):1571–1579

7. Charbonnier C, Lädermann A, Kevelham B, Chagué S, Hoffmeyer P, Holzer N (2018) Shoulder Strengthening Exercises Adapted to Specific Shoulder Pathologies Can Be Selected Using New Simulation Techniques: A Pilot Study. Int J CARS 13(2):321–330

8. Clément J, R Dumas and NH, de Guise J (2015) Soft tissue artifact compensation in knee kinematics by multi-body optimization: Performance of subject-specific knee joint models. J Biomech 48:3796–3802

9. Clément J, Dumas R, Hagemeister N, de Guise J (2017) Can generic knee joint models improve the measurement of osteoarthritic knee kinematics during squatting activity? Comput Meth Biomech Biomed Eng 20(1):94–103

10. Dragoo J, Phillips C, Schmidt J, Scanlan S, Blazek K, Steadman J, Williams A (2010) Mechanics of the anterior interval of the knee using open dynamic MRI. Clin Biomech 25:433–437

11. Duprey S, Chèze L, Dumas R (2010) Influence of joint constraints on lower limb kinematics estimation from skin markers using global optimization. J Biomech 43(14):2858–2862

12. Englander ZA, Baldwin E, Smith W, Garrett W, Spritzer C, DeFrate L (2019) In Vivo Anterior Cruciate Ligament Deformation During a Single-Legged Jump Measured by Magnetic Resonance Imaging and High-Speed Biplanar Radiography. Am J Sport Med 47(13):3166–3172

13. Gasparutto X, Sancisi N, Jacquelin E, Parenti-Castelli V, Dumas R (2015) Validation of a multi-body optimization with knee kinematic models including ligament constraints. J Biomech 48:1141–1446

14. Goyal K, Tashman S, Wang J, Li K, Zhang X, Harner C (2012) In vivo analysis of the isolated posterior cruciate ligament-deficient knee during functional activities. Am J Sports Med 40(4):777–785

15. Kim H, Seo H, Kim H, Nguyenn T, Shetty N, Yoo Y (2011) Tension Changes Within the Bundles of Anatomic Double-Bundle Anterior Cruciate Ligament Reconstruction at Different Knee Flexion Angles: A Study Using a 3-Dimensional Finite Element Model. Arthroscopy 27(10):1400–1408

16. Kim J, Lee Y, Yang B, Oh S, Yang S (2013) Rehabilitation after posterior cruciate ligament reconstruction: a review of the literature and theoretical support. Arch Orthop Trauma Surg 133(12):1687–1695

17. King AJ, Deng Q, Tyson R, Sharp JC, Matwiy J, Tomanek B, Dunn JF (2014) In Vivo Open-Bore MRI Reveals Region- and Sub-Arc-Specific Lengthening of the Unloaded Human Posterior Cruciate Ligament. PLoS One 7(11):e48,714–e48,714

18. Komatsu T, Kadoya Y, Nakagawa S, Yoshida G, Takaoka K (2005) Movement of the posterior cruciate ligament during knee flexion - MRI analysis. J Orthop Res 23:334–339

19. Laprade C, Civitarese D, Rasmussen M, Laprade R (2015) Emerging Updates on the Posterior Cruciate Ligament A Review of the Current Literature. Am J Sport Med 43(12):3077–3092

20. Leardini A, Belvedere C, Nardini F, Sancisi N, Conconi M, Parenti-Castelli V (2017) Kinematic models of lower limb joints for musculo-skeletal modelling and optimization in gait analysis. J Biomech 6(62):77–86

21. Mueller M, Heidelberger B, Hennix M, Ratcliff J (2007) Position based dynamics. J Vis Comun Image Represent 18(2):109–118

22. Nakagawa S, Johal P, Pinskerova V, Komatsu T, Sosna A, Williams A, Freeman M (2004) The posterior cruciate ligament during flexion of the normal knee. J Bone Joint Surg Br 86:450–456

23. de Paula Leite Cury R, Dan Kiyomoto H, Fogolin Rosal G, Fernandes Bryk F, Marques de Oliveira V, Arbix de Camargo O (2012) Rehabilitation protocol after isolated posterior cruciate ligament reconstruction. Rev Bras Orthop 47(4):421–427

24. Provot X (1997) Collision and self-collision handling in cloth model dedicated to design garment. In Computer Animation and Simulation'97 Springer, Vienna pp 177–189

25. Ramaniraka N, Terrier A, Theumann N, Siegrist O (2005) Effects of the posterior cruciate ligament reconstruction on the biomechanics of the knee joint: a finite element analysis. Clin Biomech 20:434–442

26. Richard V, Lamberto G, Lu T, Cappozzo A, Dumas R (2016) Knee Kinematics Estimation Using Multi-Body Optimisation Embedding a Knee Joint Stiffness Matrix: A Feasibility Study. PLOS ONE 11(6):e0157,010

27. Richard V, Cappozzo A, Dumas R (2017) Comparative assessment of knee joint models used in multi-body kinematics optimisation for soft tissue artefact compensation. J Biomech 6(62):1–7

28. Sangeux M, Marin F, Charleux F, Duerselen L, Tho MCHB (2006) Quantification of the 3D relative movement of external marker sets vs. bones based on magnetic resonance imaging. Clin Biomech 21:984–991

29. Scarvell J, Smith P, Refshauge K, Galloway H, Woods K (2004) Evaluation of a method to map tibiofemoral contact points in the normal knee using MRI. J Orthop Res 22:788–793

30. Song Y, Debski R, Musahl V, Thomas M, Woo S (2004) A three-dimensional finite element model of the human anterior cruciate ligament: a computational analysis with experimental validation. J Biomech 37(3):383–390

31. Taylor K, Terry M, Utturkar G, Spritzer C, Queen R, Irribarra L, Garrett W, DeFrate L (2011) Measurement of in vivo anterior cruciate ligament strain during dynamic jump landing. J Biomech 44(3):365–371

32. Utturkar G, Irribarra L, Taylor K, Spritzer C, Taylor D, Garrett W, Defrate LE (2013) The effects of a valgus collapse knee position on in vivo ACL elongation. Ann Biomed Eng 41(1):123–130

33. Vairis A, Stefanoudakis G, Petousis M, Vidakis N, Tsainis A, Kandyla B (2016) Evaluation of an intact, an ACL-deficient, and a reconstructed human knee joint finite element model. Comput Meth Biomech Biomed Eng 19(3):263–270

34. Wu G, Siegler S, Allard P, Kirtley C, Leardini A, Rosenbaum D, Whittle M, DLima D, Cristofolini L, Witte H, Schmid O, Strokes I (2002) ISB recommendation on definitions of joint coordinate system of various joints for the reporting of human joint motion - part I: Ankle, hip and spine. J Biomech 35(4):543–548

35. Yao J, Lancianese S, Hovinga K, Lee J, Lerner A (2008) Magnetic resonance image analysis of meniscal translation and tibio-menisco-femoral contact in deep knee flexion. J Orthop Res 26:673–684

Table 1. Length (mm) and length variation (%) of the knee ligaments at the different knee flexion angles measured based on 3D reconstructions from MRI* (n = 9)

Flexion angle	ACL		PCL_PM		PCL_AL		MCL		LCL	
	Length	**Ratio**†	**Length**	**Ratio**†	**Length**	**Ratio**†	**Length**	**Ratio**†	**Length**	**Ratio**†
0°	31.8 ± 5.0	100% ± 0%	35.2 ± 5.6	100% ± 0%	33.4 ± 5.2	100% ± 0%	91.0 ± 10.4	100% ± 0%	55.8 ± 7.3	100% ± 0%
45°	30.5 ± 5.3	96% ± 5%	37.0 ± 6.3	105% ± 6%	35.1 ± 5.9	105% ± 5%	89.1 ± 9.3	98% ± 4%	55.1 ± 6.4	99% ± 5%
90°	31.9 ± 4.8	100% ± 5%	38.4 ± 6.4	109% ± 5%	36.1 ± 5.8	108% ± 6%	86.5 ± 9.2	95% ± 6%	52.1 ± 6.0	94% ± 4%
110°	33.0 ± 3.8	106% ± 7%	36.9 ± 5.6	108% ± 6%	34.6 ± 5.4	106% ± 7%	79.1 ± 10.6	88% ± 9%	49.4 ± 5.5	89% ± 5%

* Data are mean ± SD.
† Ratio of current length with respect to the base length in neutral flexion. Percentage > 100% means that the ligament is elongated, otherwise it is shortened.

Table 2. Errors (mm) between the ligaments lengths computed by the simulation with those measured on MRI at the different knee flexion angles (n = 9)

Ligament	Mean* ± SD	Ratio** (mean ± SD)
ACL	2.1 ± 1.2	7% ± 4%
PCL_PM	2.3 ± 0.9	7% ± 2%
PCL_AL	2.0 ± 1.1	6% ± 4%
MCL	1.1 ± 1.3	1% ± 2%
LCL	2.0 ± 1.7	4% ± 3%

* Values are positive, meaning that the simulation tended to overestimate the length
** Error reported as length variation (ratio of current length with respect to the base length in neutral flexion)

Table 3. Length (mm) and length variation (%) of the knee ligaments during the dynamic activities, with indication of the knee flexion angles when the measures where taken*

Activities	Flexion angle	ACL		PCL_PM		PCL_AL		MCL		LCL	
		Length	**Ratio†**	**Length**	**Ratio†**	**Length**	**Ratio†**	**Length**	**Ratio†**	**Length**	**Ratio†**
Sitting	121.8 ± 12.2	35.5 ± 4.1	112% ± 8%	42.2 ± 7.1	116% ± 10%	39.7 ± 6.3	119% ± 10%	80.9 ± 9.2	88% ± 10%	51.4 ± 6.6	93% ± 10%
Cutting	74.5 ± 8.0	35.0 ± 4.6	108% ± 14%	41.2 ± 6.9	114% ± 12%	38.4 ± 6.0	115% ± 10%	91.9 ± 8.8	101% ± 5%	55.4 ± 5.5	100% ± 5%
Drop jump	106.2 ± 23.1	35.7 ± 4.3	113% ± 8%	42.1 ± 7.7	116% ± 2%	39.3 ± 7.0	118% ± 9%	84.9 ± 8.3	94% ± 8%	53.5 ± 4.9	97% ± 7%
Kangaroo jump	126.1 ± 15.5	35.6 ± 3.5	115% ± 10%	42.1 ± 7.9	117% ± 10%	40.1 ± 8.4	123% ± 12%	83.9 ± 6.3	93% ± 6%	53.6 ± 4.3	99% ± 11%
Sidestepping	71.3 ± 11.3	34.7 ± 4.6	109% ± 5%	40.5 ± 7.2	111% ± 12%	38.1 ± 6.1	114% ± 9%	92.3 ± 9.2	102% ± 4%	52.5 ± 9.3	95% ± 17%

* Data are mean ± SD and reported for the participants performing three trials for each activity.
† Ratio of current length with respect to the base length in neutral flexion. Percentage > 100% means that the ligament is elongated, otherwise it is shortened.